IFAC Journal of Systems and Control 35 (2026) 100387

Contents lists available at ScienceDirect

IFAC Journal of Systems and Control

journal homepage: www.elsevier.com/locate/ifacsc

Full length article

Qualitative behavior analysis of a model underlying the Warburg effect☆

Pasquale Palumbo [a,b,c,*], Susanna Brotti [a], Raghvendra Singh [d]

[a] Department of Biotechnology and Biosciences, University of Milano-Bicocca, Piazza della Scienza 2, 20126 Milan, Italy
[b] SYSBIO Centre for Systems Biology, Milan, Italy
[c] Institute for Systems Analysis and Computer Science "A. Ruberti", National Research Council (IASI-CNR), Via dei Taurini, 19, 00185 Rome, Italy
[d] Department of Chemical Engineering, Indian Institute of Technology Kanpur, Kanpur 208016, India

ARTICLE INFO

Article history:
Received 31 October 2025
Received in revised form 23 January 2026
Accepted 4 February 2026
Available online 16 February 2026

Keywords:
Biomedical system modeling
Identification
Simulation

ABSTRACT

The Warburg effect describes the preference of highly proliferating cells (like cancer cells) for aerobic glycolysis and lactate production despite oxygen availability. In a recent paper, Jaiswal and Singh (2024) proposed that this behavior arises from a negative feedback loop linking cytoplasmic NADH levels and cell proliferation. Their model integrates glycolysis, oxidative phosphorylation, and pyruvate-to-lactate conversion to explain how the NADH/NAD+ ratio governs proliferation and quiescence. Here, we propose the qualitative behavior analysis, showing how quiescent and non quiescent equilibria arise according to model parameters. The corresponding bifurcation diagrams provide new biological insights on cellular behavior and pave the way to further investigation on the cellular machinery leading to the Warburg effect.

1. Introduction

The metabolic reprogramming of cancer cells, known as the Warburg effect, represents one of the fundamental hallmarks of tumor metabolism. Otto Heinrich Warburg first observed that, unlike normal cells, cancer cells preferentially ferment glucose into lactate even in the presence of oxygen, a process termed aerobic glycolysis, Warburg (1956). Although complete oxidation of glucose through the tricarboxylic acid (TCA) cycle and oxidative phosphorylation (OXPHOS) is energetically more efficient, aerobic glycolysis is a general feature of proliferating cells, both cancerous and normal, Vander Heiden et al. (2009) and Liberti and Locasale (2016).

During glycolysis, glucose oxidation produces NADH. To sustain glycolytic flux, NAD+ must be continuously regenerated from NADH. This regeneration occurs via three main mechanisms: the malate–aspartate shuttle (MAS), the glycerol 3-phosphate shuttle (G3PS), and the reduction of pyruvate to lactate by lactate dehydrogenase (LDH) (De Leon-Oliva et al., 2025; Wang et al., 2022). While MAS and G3PS transfer reducing equivalents into mitochondria to fuel OXPHOS, the LDH reaction enables glycolysis to proceed independently of mitochondrial activity. The recent observation that mitochondrial NADH shuttles become saturated during rapid proliferation suggests that this saturation contributes to driving the Warburg effect (Wang et al., 2022).

Accumulation of cytosolic NADH, or limited mitochondrial NADH oxidation capacity, can push cells toward lactate production as a mechanism to restore redox equilibrium (Papaneophytou, 2024). This highlights that the Warburg effect is not merely a metabolic byproduct but rather a finely tuned adaptation that regulates NADH turnover and maintains NAD+ availability for both glycolysis and biosynthetic reactions. However, the precise mechanism by which lactate production promotes proliferation, and how aerobic glycolysis interacts with OXPHOS, remains incompletely understood. In Alberghina (2023), the Warburg effect is interpreted not as a defect in energy production, but as an adaptive metabolic strategy that enables fast-growing cells to redirect resources toward biosynthesis. It emerges from the integration between enhanced glycolysis and heterogeneous mitochondrial function, providing a systems-level view of cancer metabolism.

In Jaiswal and Singh (2024), it is proposed that the Warburg effect arises from a double negative/positive feedback loop between cytoplasmic NADH concentration and the rate of cell proliferation: from the one hand, NADH concentration acts as a positive feedback on the proliferation rate; from the other hand, the proliferation rate acts as an inhibitor of NADH accumulation rate. Despite the minimal structure of the model, it is able to account for mechanisms underlying cell quiescence, a typical response observed in cancer stem cells that contributes

☆ This article is part of a Special issue entitled: 'IFAC WC 2026 - TC 8.2' published in IFAC Journal of Systems and Control.

* Corresponding author at: Department of Biotechnology and Biosciences, University of Milano-Bicocca, Piazza della Scienza 2, 20126 Milan, Italy.
E-mail address: pasquale.palumbo@unimib.it (P. Palumbo).

https://doi.org/10.1016/j.ifacsc.2026.100387

to drug resistance (Chen et al., 2016; Lee et al., 2020). The regulatory architecture of our NADH-proliferation model may be connected to other biological decision-making modules characterized by coupled feedback interactions. For instance, with the Ime1–Ime2 regulatory system in yeast, which governs the irreversible commitment to meiosis through a transcriptional cascade and feedback-controlled switching dynamics, Smith et al. (1990) and Guttmann-Raviv et al. (2002). From a Systems & Control perspective, both systems can be interpreted as feedback-driven switches regulating transitions between mutually exclusive cellular states.

The model in Jaiswal and Singh (2024) had been used to study the impact of a shift in the redox ratio (NADH/NAD+ ratio) on cell proliferation, occurring during the metabolic reprogramming of cancer cells. In the present work, we have studied the impact of different parameters on the switching of the cell state from proliferation to quiescence, by performing a stability analysis of the equilibrium points. Bifurcation diagrams are reported to highlight the role of different parameters in the quiescence/non-quiescence switch: since each model parameter is closely related to a biological function, variations in their values provide insights into how specific molecular or cellular processes can drive transitions between resting and active states. The novelty of the present contribution lies in providing a qualitative behavior analysis that was lacking in Jaiswal and Singh, 2024. Specifically, we complement the original modeling framework with a systematic qualitative analysis that allows us to characterize equilibrium points, their stability properties, and the asymptotic behavior of the system as a function of biologically meaningful parameters.

The paper is organized as follows. Section 2 summarizes the dynamics of the model proposed in Jaiswal and Singh (2024). Section 3 presents the qualitative behavior analysis, providing conditions for the existence and stability of biologically meaningful equilibria. Sections 4 and 5 report the bifurcation diagrams and some numerical simulations, respectively. Conclusions are drawn in Section 5.

2. Model formulation

The model presented in Jaiswal and Singh (2024) consists of a two-dimensional system of Ordinary Differential Equations describing the dynamics of the cell proliferation rate C_p, which is tightly coupled to the NADH concentration N:

$$\begin{cases} \dfrac{dC_p}{dt} = k_1 \dfrac{N}{k_2 + N} C_p - k_{d1} C_p \\ \dfrac{dN}{dt} = \dfrac{k_3}{k_4 + C_p} - k_{d2} N \end{cases} \tag{1}$$

Regarding the cell proliferation dynamics (C_p), its growth rate is positively regulated by N through a monotonically increasing Michaelis–Menten saturating function. In this formulation k_1 represents the maximum proliferation rate coefficient (achieved for large values of N), while k_2 denotes the NADH concentration at which the proliferation rate reaches half of its maximum. The saturating function accounts for the dual role of NADH: for low NADH concentrations ($N \ll k_2$), the proliferation rate increases almost linearly with N, with proportionality coefficient k_1/k_2, corresponding to the maximum cell division rate (k_1) divided by the basal level of apoptosis (k_2). For high NADH concentrations ($N \gg k_2$), the effect of NADH-dependent apoptosis causes the rate to saturate toward k_1, becoming progressively less sensitive to further increases in N. In addition, the cell cycle-dependent apoptosis contributes to reducing proliferation at a rate k_{d1}.

On the other hand, the NADH production rate is negatively regulated by the proliferation rate C_p, following a monotonically decreasing Michaelis–Menten function. Here, k_3/k_4 denotes the maximum NADH production rate (achieved in quiescent cells, i.e. $C_p = 0$), and k_4 is the value of C_p corresponding to half of the maximal NADH production rate.

Biologically, k_3 represents the NADH flux from glycolysis, while k_4 determines the saturation behavior, reflecting the reduction in NADH production due to the pyruvate-to-lactate conversion that characterizes aerobic glycolysis. The NADH balance is further regulated by its mitochondrial consumption, modeled as a linear flux with rate constant k_{d2}. Within this framework, cells exhibiting the Warburg effect, an enhanced conversion of pyruvate to lactate despite the presence of oxygen, are represented by an increase in k_4, indicating a reduced mitochondrial contribution to NADH oxidation.

Comprehensive descriptions of all model parameters and their biological interpretations are provided in Jaiswal and Singh (2024) and references therein.

Remark 1. Since C_p is defined as the cell proliferation rate, it may assume positive values (for non-quiescent, growing cells), null value (for non-growing, quiescent cells) or negative values (for apoptotic cells). Instead, model parameters and initial conditions need to be chosen so as to ensure non-negative evolutions of the NADH concentration.

3. Qualitative behavior analysis

3.1. Equilibrium points

The system has two equilibrium points. One is for *quiescent cells* (i.e. with $C_p = 0$):

$$C_{p,q} = 0, \qquad N_q = \frac{k_3}{k_4 k_{d2}} \tag{2}$$

Since N_q is always positive (as all parameters are strictly positive), the quiescent equilibrium exists and is biologically meaningful for any choice of model parameters in the positive orthant.

Remark 2. Cells exhibiting the Warburg effect display a smaller quiescent NADH steady-state value due to their higher k_4 parameter.

The other equilibrium point is for *non-quiescent* cells (i.e. with $C_p \neq 0$):

$$\begin{aligned} N_{nq} &= \frac{k_{d1} k_2}{k_1 - k_{d1}}, \\ C_{p,nq} &= \frac{k_3}{k_{d2} N_{nq}} - k_4 = \frac{k_3(k_1 - k_{d1}) - k_{d1} k_{d2} k_2 k_4}{k_{d1} k_{d2} k_2} \end{aligned} \tag{3}$$

This non-quiescent equilibrium is biologically meaningful only if $N_{nq} > 0$, that means:

$$N_{nq} = \frac{k_{d1} k_2}{k_1 - k_{d1}} > 0 \qquad \Longleftrightarrow \qquad k_1 > k_{d1} \tag{4}$$

Besides, provided that $k_1 > k_{d1}$, we have positive growth if

$$C_{p,nq} = \frac{k_3(k_1 - k_{d1}) - k_{d1} k_{d2} k_2 k_4}{k_{d1} k_{d2} k_2} > 0 \tag{5}$$

that is

$$\frac{k_{d1} k_2}{k_1 - k_{d1}} < \frac{k_3}{k_4 k_{d2}} \tag{6}$$

Otherwise, if inequality (6) is not satisfied, then $C_{p,nq} < 0$, meaning that the cell population declines to zero. It is worth noting that inequality (6) can be equivalently expressed in terms of the quiescent and non-quiescent stationary NADH values:

$$0 < \frac{k_{d1} k_2}{k_1 - k_{d1}} = N_{nq} < \frac{k_3}{k_4 k_{d2}} = N_q \tag{7}$$

In other words, the non-quiescent equilibrium exists and means positive growth if the non-quiescent NADH equilibrium N_{nq} is positive and smaller than the stationary NADH provided by the quiescent equilibrium N_q.

Otherwise, if

$$N_{nq} > \frac{k_3}{k_4 k_{d2}} = N_q \tag{8}$$

then $C_{p,nq} < 0$.

Finally, if $N_{nq} < 0$ (i.e. if $k_1 < k_{d1}$), then, from (3) it comes that $C_{p,nq} < 0$ as well. However, we stress that such an equilibrium point has a pure mathematical meaning.

Remark 3. The stationary NADH concentrations for quiescent and non-quiescent cells depend on orthogonal sets of model parameters, since the ones that set N_q, namely k_3, k_4 and k_{d2} that refer to NADH dynamics, are different from the ones that set N_{nq}, namely k_1, k_2 and k_{d1}, the ones that refer to C_p dynamics. As a matter of fact, by fixing $\{k_3, k_4, k_{d2}\}$, $C_{p,nq}$ is forced to live on the manifold

$$C_{p,nq} = \frac{k_3}{k_{d2} N_{nq}} - k_4, \tag{9}$$

where N_{nq} is free to vary because of $\{k_1, k_2, k_{d1}\}$.

Remark 4. According to (4), the Warburg effect does not influence the value of N_{nq}, whereas it affects $C_{p,nq}$ as described in (9): an increase in the pyruvate-to-lactate flux, represented by a higher k_4, directly reduces the stationary proliferation rate.

In summary:

- if:

$$0 < N_{nq}(k_1, k_2, k_{d1}) < N_q(k_3, k_4, k_{d2}) \tag{10}$$

  then, we have both quiescent and non-quiescent equilibrium points in the positive orthant, with the non-quiescent point meaning positive growth;
- if

$$N_{nq}(k_1, k_2, k_{d1}) > N_q(k_3, k_4, k_{d2}) \tag{11}$$

  then, we have both the quiescent and non-quiescent equilibrium points in the positive orthant, but the non-quiescent point here means negative growth;
- if

$$N_{nq}(k_1, k_2, k_{d1}) < 0 \tag{12}$$

  then, we have only the quiescent point in the positive orthant.

3.2. Stability analysis

Stability analysis is carried out by evaluating the Jacobian matrix:

$$J = \begin{bmatrix} k_1 \dfrac{N}{k_2 + N} - k_{d1} & k_1 \dfrac{k_2}{(k_2 + N)^2} C_p \\ -\dfrac{k_3}{(k_4 + C_p)^2} & -k_{d2} \end{bmatrix} \tag{13}$$

At the quiescent equilibrium, the Jacobian becomes:

$$J_q = \begin{bmatrix} k_1 \dfrac{N_q}{k_2 + N_q} - k_{d1} & 0 \\ -\dfrac{k_3}{k_4^2} & -k_{d2} \end{bmatrix} \tag{14}$$

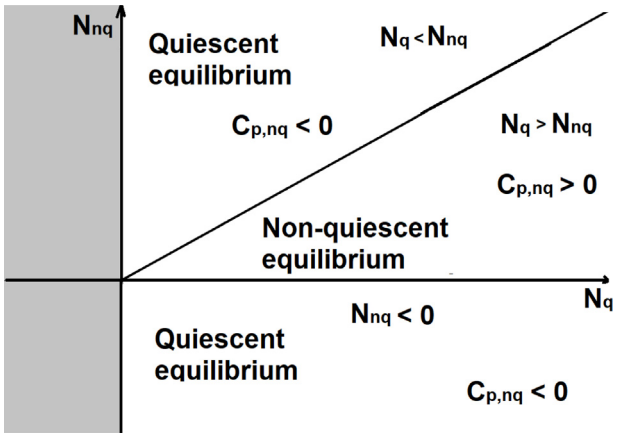

Fig. 1. Regions of asymptotic stability for the quiescent and non-quiescent equilibria in the N_q–N_{nq} positive orthant.

so that stability is ensured if

$$k_1 \frac{N_q}{k_2 + N_q} < k_{d1} \quad \Longleftrightarrow \quad (k_1 - k_{d1}) N_q < k_2 k_{d1} \tag{15}$$

If $k_1 < k_{d1}$ (i.e., $N_{nq} < 0$), inequality (15) is satisfied regardless of the other parameter values, and the quiescent equilibrium is asymptotically stable. Conversely, if $k_1 > k_{d1}$ (i.e., $N_{nq} > 0$), asymptotic stability is guaranteed provided that

$$N_q < \frac{k_2 k_{d1}}{k_1 - k_{d1}} = N_{nq} \tag{16}$$

In summary, the quiescent equilibrium is asymptotically stable if, and only if, the stationary value $C_{p,nq}$ of the non-quiescent equilibrium is negative.

At the non-quiescent equilibrium, the Jacobian is

$$J_{nq} = \begin{bmatrix} 0 & \dfrac{k_1 k_2 C_{p,nq}}{(k_2 + N_{nq})^2} \\ \dfrac{k_3}{(k_4 + C_{p,nq})^2} & -k_{d2} \end{bmatrix} \tag{17}$$

The characteristic polynomial of J_{nq} is

$$p(\lambda) = \lambda^2 + k_{d2}\lambda + \frac{k_1 k_2 k_3}{(k_2 + N_{nq})^2 (k_4 + C_{p,nq})^2} C_{p,nq} \tag{18}$$

According to the Routh–Hurwitz criterion, if $C_{p,nq} > 0$, all coefficients are positive, implying that the non-quiescent equilibrium is asymptotically stable. Conversely, if $C_{p,nq} < 0$, not all roots have negative real parts, and the equilibrium is unstable.

In summary:

- if inequality (10) holds, both quiescent and non-quiescent equilibria exist in the positive orthant: the quiescent equilibrium is unstable, and the non-quiescent equilibrium is asymptotically stable, providing positive proliferation rate;
- otherwise, if either inequality (11) or (12) holds, only the quiescent equilibrium is asymptotically stable.

The emergence of the quiescent and non-quiescent asymptotically stable equilibria is summarized in Fig. 1.

4. Bifurcation diagrams

To investigate the qualitative behavior of the system, we consider bifurcation diagrams for different model parameters, focusing on the stationary proliferation rate C_p. As usual, continuous lines indicate asymptotic stability, whereas dashed lines indicate

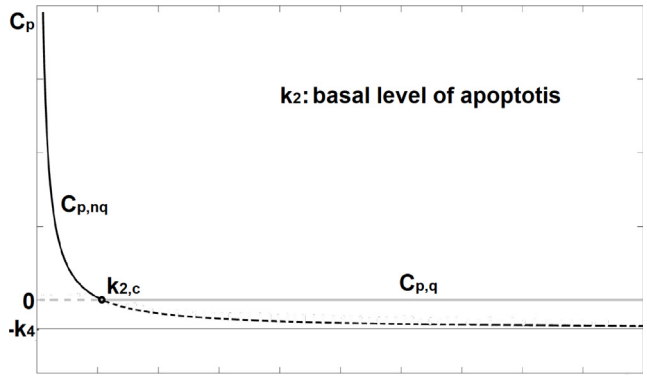

Fig. 2. Bifurcation diagram for parameter k_2. Gray line: quiescent equilibrium; black line: non-quiescent equilibrium.

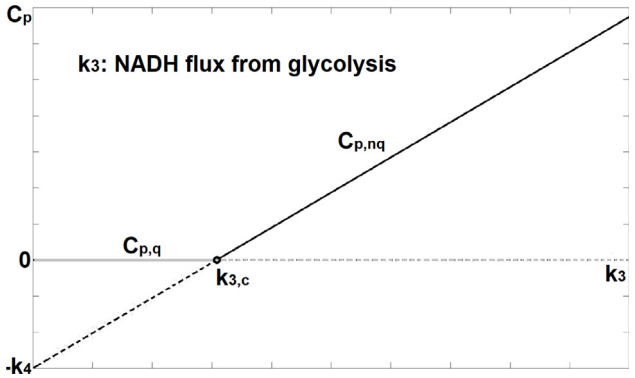

Fig. 3. Bifurcation diagram for parameter k_3. Gray line: quiescent equilibrium; black line: non-quiescent equilibrium.

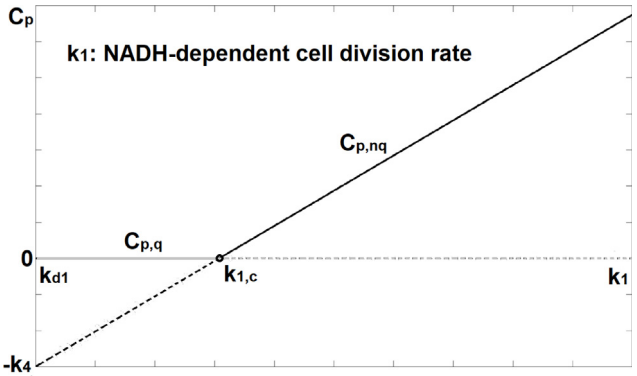

Fig. 4. Bifurcation diagram for parameter k_1. Gray line: quiescent equilibrium; black line: non-quiescent equilibrium.

instability. These diagrams are derived from the non-quiescent equilibrium formula reported in (3) for positive values of C_p. They all show a classical transcritical bifurcation behavior since, by varying the bifurcation parameter, there always exist 2 stationary points (one stable, the other unstable), whose stability is interchanged by crossing a specific critical value, Strogatz (2000), Wiggins (1990).

Variation of k_2: Fig. 2 shows the effect of varying parameter k_2, which represents the NADH-independent apoptosis. As k_2 varies in $(0, +\infty)$, the quiescent equilibrium remains unchanged, whereas the non-quiescent equilibrium varies. Assuming $N_{nq} > 0$ (i.e., $k_1 > k_{d1}$), low values of k_2 correspond to $C_{p,nq} > 0$, so that inequality (10) is satisfied and the cell exhibits an asymptotically stable positive proliferation rate. By increasing k_2, from (3) a critical value

$$k_{2,c} = \frac{k_3(k_1 - k_{d1})}{k_{d1}k_{d2}k_4}, \tag{19}$$

is reached, above which the asymptotic stability of $C_{p,nq}$ is lost and the cell switches to the asymptotically stable quiescent state.

Variation of k_{d2}: A bifurcation pattern similar to that in Fig. 2 is observed when varying k_{d2}, which corresponds to the NADH flux to mitochondria. As k_{d2} varies in $(0, +\infty)$, both the quiescent and non-quiescent equilibria change. Assuming $N_{nq} > 0$ (i.e., $k_1 > k_{d1}$), low values of k_{d2} correspond to $C_{p,nq} > 0$, so that inequality (10) is satisfied and the cell exhibits an asymptotically stable positive proliferation rate. By increasing k_{d2}, from (3) a critical value

$$k_{d2,c} = \frac{k_3(k_1 - k_{d1})}{k_{d1}k_2k_4}, \tag{20}$$

is reached, above which the asymptotic stability of $C_{p,nq}$ is lost and the cell switches to the asymptotically stable quiescent state. Unlike the case of k_2, here the stationary NADH value at the quiescent equilibrium decreases as k_{d2} is further increased.

Variation of k_3: Fig. 3 shows the effect of varying parameter k_3, the NADH flux from glycolysis. As k_3 varies in $(0, +\infty)$, both the quiescent and non-quiescent equilibria change. Assuming $N_{nq} > 0$ (i.e., $k_1 > k_{d1}$), high values of k_3 correspond to $C_{p,nq} > 0$, so that inequality (10) is satisfied and the cell exhibits an asymptotically stable positive proliferation rate. By decreasing k_3, a critical value

$$k_{3,c} = \frac{k_{d1}k_{d2}k_2k_4}{k_1 - k_{d1}}, \tag{21}$$

is reached, below which the asymptotic stability of $C_{p,nq}$ is lost and the cell switches to the asymptotically stable quiescent state. In this case, the stationary NADH concentration at the quiescent equilibrium decreases as k_3 is further reduced.

Variation of k_1: Fig. 4 shows the effect of varying parameter k_1, the proliferation rate due to NADH. As k_1 varies in $(k_{d1}, +\infty)$, the quiescent equilibrium remains unchanged, whereas the non-quiescent equilibrium changes. The range of variation of k_1 ensures that $N_{nq} > 0$ (i.e., $k_1 > k_{d1}$). High values of k_1 correspond to $C_{p,nq} > 0$, so that inequality (10) is satisfied and the cell exhibits an asymptotically stable positive proliferation rate. By decreasing k_1, a critical value

$$k_{1,c} = \frac{k_{d1}k_{d2}k_2k_4}{k_3} + k_{d1}, \tag{22}$$

is reached, below which the asymptotic stability of $C_{p,nq}$ is lost and the cell switches to the asymptotically stable quiescent state.

Variation of k_{d1}: Fig. 5 shows the effect of varying parameter k_{d1}, the proliferation rate due to NADH. As k_{d1} varies in $(0, k_1)$, the quiescent equilibrium remains unchanged, whereas the non-quiescent equilibrium changes. The range of variation of k_{d1} ensures that $N_{nq} > 0$ (i.e., $k_1 > k_{d1}$). Low values of k_{d1} correspond to $C_{p,nq} > 0$, so that inequality (10) is satisfied and the cell exhibits an asymptotically stable positive proliferation rate. By increasing k_{d1}, a critical value

$$k_{d1,c} = k_1 - \frac{k_{d1}k_{d2}k_2k_4}{k_3}, \tag{23}$$

is reached, above which the asymptotic stability of $C_{p,nq}$ is lost and the cell switches to the asymptotically stable quiescent state.

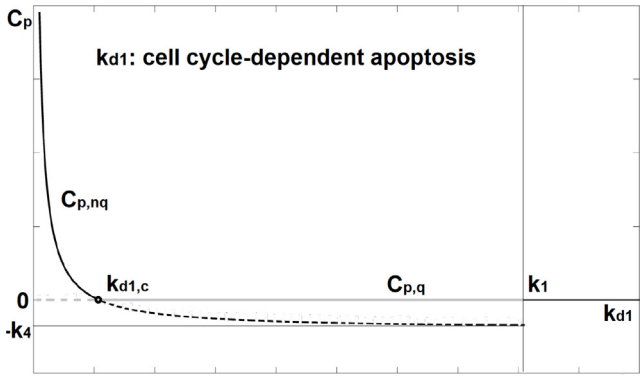

Fig. 5. Bifurcation diagram for parameter k_{d1}. Gray line: quiescent equilibrium; black line: non-quiescent equilibrium.

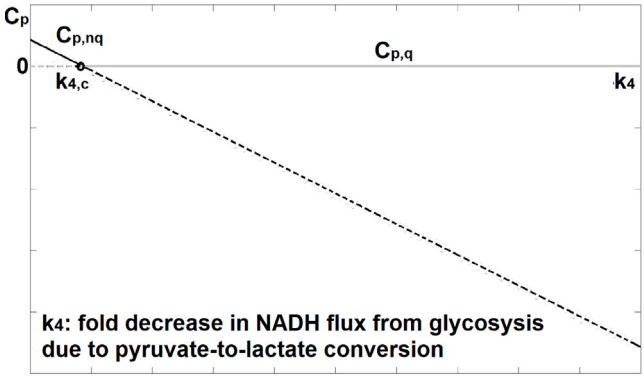

Fig. 6. Bifurcation diagram for parameter k_4. Gray line: quiescent equilibrium; black line: non-quiescent equilibrium.

Variation of k_4: Fig. 6 shows the effect of varying parameter k_4, representing the fold reduction in NADH due to lactate production. As k_4 varies in $(0, +\infty)$, both the quiescent and non-quiescent equilibria change. Assuming $N_{nq} > 0$ (i.e., $k_1 > k_{d1}$), low values of k_4 correspond to $C_{p,nq} > 0$, so that inequality (10) is satisfied and the cell exhibits an asymptotically stable positive proliferation rate. By increasing k_4, from (3) a critical value

$$k_{4,c} = \frac{k_3(k_1 - k_{d1})}{k_{d1}k_{d2}k_2}, \tag{24}$$

is reached, below which the asymptotic stability of $C_{p,nq}$ is lost and the cell switches to the asymptotically stable quiescent state. In this case, the stationary NADH concentration at the quiescent equilibrium decreases as k_4 is further increased.

Finally, Fig. 7 shows the proliferation rate as a function of the stationary NADH concentration from (3), illustrating the switch between non-quiescent and quiescent states. Once the NADH machinery is fixed (i.e., the parameters k_3, k_4, and k_{d2} are held constant), an increase of N above the threshold N_q triggers the transition from the non-quiescent to the quiescent state. Since the Warburg effect promotes pyruvate-to-lactate conversion (i.e., increases k_4), the quiescent stationary value N_q decreases, so that smaller NADH concentrations are sufficient to induce quiescence in tumor cells.

5. Numerical simulations

Simulations are carried out according to the following non-dimensionalized version of the model, in order to deal with meaningful evolutions without addressing the identification task: indeed, the numerical simulations are meant to illustrate the qualitative analysis and should not be interpreted as predictive results. To this end we define the normalized state variables

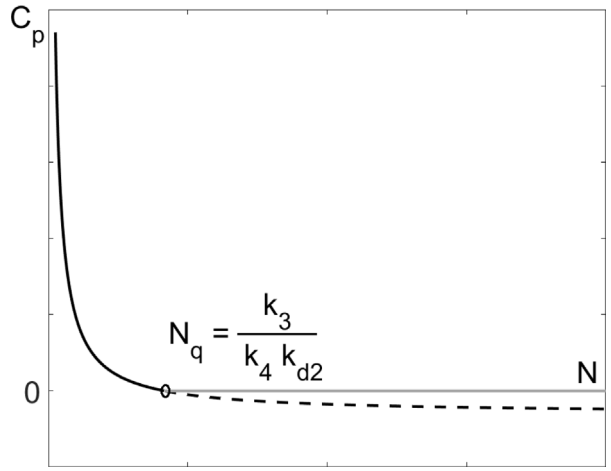

Fig. 7. Proliferation rate C_p as a function of stationary NADH concentration N. Gray line: quiescent equilibrium; black line: non-quiescent equilibrium.

$$\overline{C_p} = C_p/k_4, \qquad \overline{N} = N/k_2 \tag{25}$$

and consider their variations with respect to the cell cycle fraction $\tau = t/T$, where T is the cell cycle length. Therefore, the system in (1) may be rewritten as:

$$\begin{cases} \dfrac{d\overline{C_p}}{d\tau} = D_c\left(\overline{k_1}\dfrac{\overline{N}}{1+\overline{N}}\overline{C_p} - \overline{C_p}\right) \\ \dfrac{d\overline{N}}{d\tau} = D_N\left(\dfrac{\Gamma}{1+\overline{C_p}} - \overline{N}\right) \end{cases} \tag{26}$$

with

$$\overline{k_1} = \frac{k_1}{k_{d1}}, \quad D_c = k_{d1}T, \quad D_N = k_{d2}T, \quad \Gamma = \frac{k_3}{k_2k_4k_{d2}} \tag{27}$$

To make simulations we set $D_c = 1$ and $D_N \gg D_c$ to account for the fact that NADH dynamics is faster than C_p dynamics. Unless differently specified in the figures, the chosen non-dimensionalized parameters are below reported

$$\overline{k_1} = 2.12, \qquad \Gamma = 10, \qquad D_N = 50$$

According to these values, inequality (10) ensuring the asymptotic stability of the non-quiescent equilibrium point is satisfied, as well as a positive stationary proliferation rate.

Figs. 8–9 show that, by increasing $\overline{k_1}$ (e.g. by increasing the NADH-dependent rate of cell proliferation), cell proliferation increases and the NADH response has a pulse form. The NADH decline after the peak is faster for higher cell proliferation, Fig. 8, according to the Warburg effect in which lactate production and mitochondria collaborate to decrease the NADH concentration, Wang et al. (2022). Further, cell proliferation declines if NADH concentration increases after reaching the peak since in that case the higher NADH causes cell cycle-dependent apoptosis. Notice that, for a very low value of $\overline{k_1}$, $\overline{C_{p,nq}}$ becomes negative. The phase portrait is reported in Fig. 10.

Figs. 11–12 show that, by increasing D_N (e.g. by increasing the rate constant of NADH flux toward oxidative phosphorylation), cell proliferation does not seem affected by changes, as well as the decline of NADH after the peak, corroborating that the decline in NADH after reaching the peak is responsible for the increase in cell proliferation. The phase portrait is reported in Fig. 13.

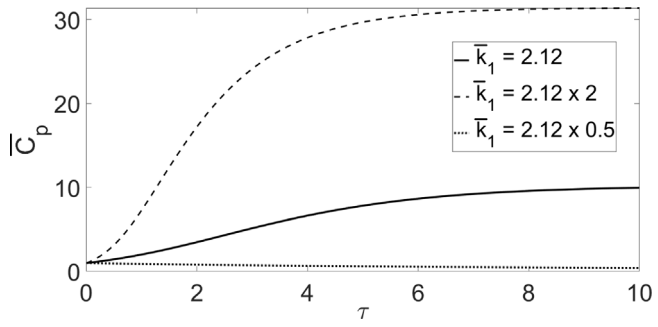

Fig. 8. $\overline{C_p}$ evolution for different values of $\overline{k_1}$.

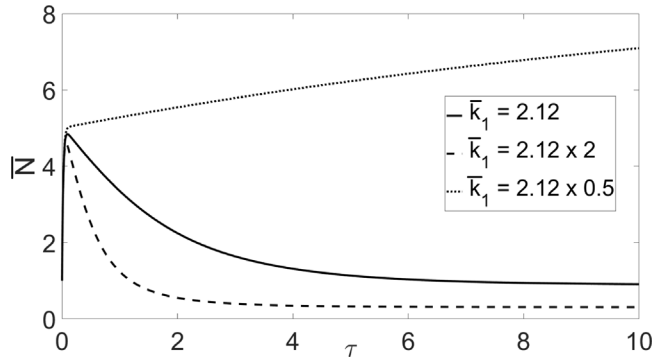

Fig. 9. $\overline{N}$ evolution for different values of $\overline{k_1}$.

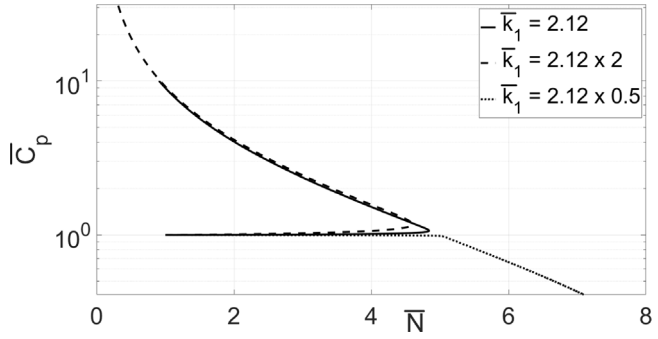

Fig. 10. Phase portrait for different values of $\overline{k_1}$.

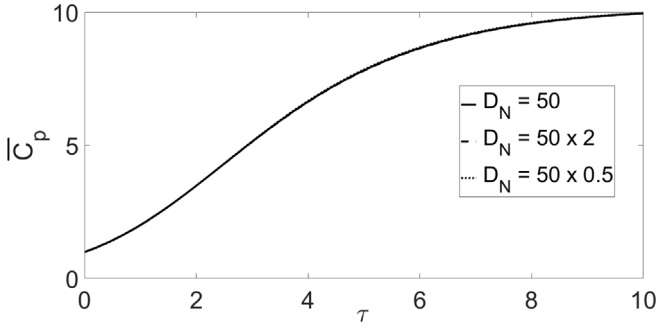

Fig. 11. $\overline{C_p}$ evolution for different values of D_N.

6. Conclusions and future work

In this work, we performed a qualitative analysis of a mathematical model describing the dynamic interplay between cell proliferation and NADH concentration. Our results demonstrate that a cell can transition between a stationary non-quiescent and a stationary quiescent state depending on variations in model parameters. This bifurcation behavior provides a dynamical interpretation of the Warburg effect, which characterizes the preference of highly proliferating cells for aerobic glycolysis and lactate production. In particular, an increase in parameter k_4, representing the pyruvate-to-lactate flux, enhances the sensitivity of cells to small changes in NADH levels.

The present model assumes single-step processes leading to the Michaelis–Menten formalism. Future extensions will incorporate two-step processes to introduce cooperativity in the regulation of cell proliferation and NADH production. Such an enhanced model is expected to display richer dynamical behaviors, including bistability and oscillations, thereby offering deeper insights into the regulatory mechanisms underlying metabolic reprogramming in proliferating cells.

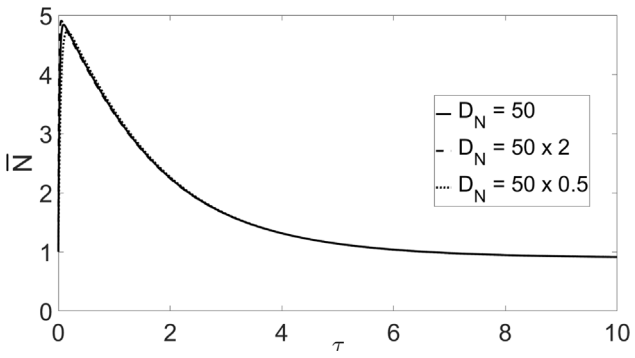

Fig. 12. $\overline{N}$ evolution for different values of D_N.

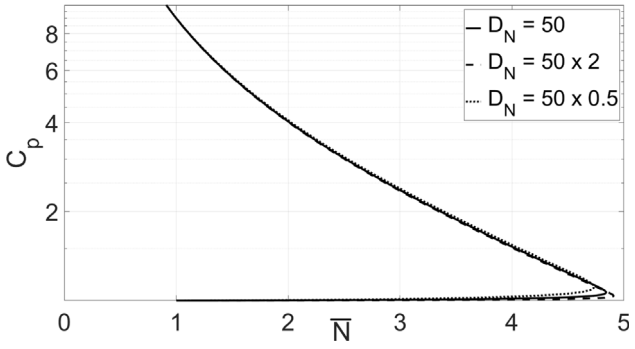

Fig. 13. Phase portrait for different values of D_N.

CRediT authorship contribution statement

Pasquale Palumbo: Writing – review & editing, Writing – original draft, Validation, Supervision, Software, Methodology, Investigation, Formal analysis, Conceptualization. **Susanna Brotti:** Software, Methodology, Investigation. **Raghvendra Singh:** Writing – review & editing, Investigation, Conceptualization.

Declaration of competing interest

The authors declare that they have no known competing financial interests or personal relationships that could have appeared to influence the work reported in this paper.

References

Alberghina, L. (2023). The warburg effect explained: Integration of enhanced glycolysis with heterogeneous mitochondria to promote cancer cell proliferation. *International Journal of Molecular Sciences*, *24*, 15787.

Chen, W., Dong, J., Haiech, J., Kilhoffer, M., & Zeniou, M. (2016). Cancer stem cell quiescence and plasticity as major challenges in cancer. *Stem Cells Int*, *1740936*.

De Leon-Oliva, D., et al. (2025). Revisiting the biological role of the warburg effect: Evolving perspectives on cancer metabolism. *Pathology, Research and Practice*, *273*, 156151.

Guttmann-Raviv, N., Martin, S., & Kassir, Y. (2002). Ime2, a meiosis-specific kinase in yeast, is required for destabilization of its transcriptional activator, Ime1. *Molecular and Cellular Biology*, *22*(7), 2047–2056.

Jaiswal, A., & Singh, R. (2024). A negative feedback loop underlies the warburg effect. *NPJ Syst. Biol. Appl.*, *10*, 55.

Lee, S., Reed-Newman, T., Anant, S., & Ramasamy, T. (2020). Regulatory role of quiescence in the biological function of cancer stem cells. *Stem Cell Rev. Rep.*, *16*, 1185–1207.

Liberti, M., & Locasale, J. (2016). The warburg effect: How does it benefit cancer cells? *Trends in Biochemical Sciences*, *41*(3).

Papaneophytou, C. (2024). The warburg effect: Is it always an enemy? *Frontiers in Bioscience*, *29*(12), 402.

Smith, H., Su, S., Neigeborn, L., Driscoll, S., & Mitchell, A. (1990). Role of IME1 expression in regulation of meiosis in *Saccharomyces cerevisiae*. *Molecular and Cellular Biology*, *10*(12), 6103–6113.

Strogatz, S. (2000). *Nonlinear Dynamics and Chaos: with Applications to Physics, Biology, Chemistry, and Engineering* (second ed.). Westview Press..

Vander Heiden, M. G., Cantley, L. C., & Thompson, C. B. (2009). Understanding the warburg effect: The metabolic requirements of cell proliferation. *Science*, *324*, 1029–1033. http://dx.doi.org/10.1126/science.1160809.

Wang, Y., et al. (2022). Saturation of the mitochondrial NADH shuttles drives aerobic glycolysis in proliferating cells. *Molecular Cell*, *82*, 3270–3283.e9. http://dx.doi.org/10.1016/j.molcel.2022.06.011.

Warburg, O. H. (1956). On the origin of cancer cells. *Science*, *123*, 309–314. http://dx.doi.org/10.1126/science.123.3191.309.

Wiggins, S. (1990). *Introduction to Applied Nonlinear Dynamical Systems and Chaos*. New York: Springer-Verlag.